Morpho-tectonic Analysis of an Upstream Sub-basin of the Cauvery River from Bhagamandala to Shivanasamudra using Geomorphic Indices using GIS

M. Samarth Urs[1]*, P. Nagendra[1], C. Vinay[1], B.V. Suresh Kumar[1], K.N. Prakash Narasimha [1]
[1]DOS in Earth Science, University of Mysore
*Corresponding author email: samarthmurs@gmail.com

(Received on 31 January 2025; In final form on 14 August 2025)

DOI: https://doi.org/10.58825/jog.2025.19.2.202

Abstract: The Cauvery sub-basin, with an elevation of 2029 meters, is a mountain range that has been uplifted during the Cretaceous period and is bordered by the Western Ghats. The two northern mountain fronts and the southern front of the Cauvery sub-basin are defined by faults near the origin point (catchment area). We conducted a morpho-tectonic analysis by assessing the properties of geomorphic indices to uncover variations in rock uplift. In particular, the study contrasts the northern and southern mountain fronts' valley height to floor ratio, area-height correlations (hypsometric curve), and mountain front sinuosity (Smf). The high land in the sub-basin and key faults in the northern part of the Western Ghats (with an average height of approximately 2029 meters), indicate the uplift of both geomorphic units as part of a single extensive crustal block. The asymmetry factor indicates that there are imbalances in the Cauvery River, with an increased slope toward the sub-basin's left side. Transverse topographic symmetry also suggests that the sub-basin experiences tectonic activity at both the source and endpoint, where Shivanasamudra falls is located. Likewise, other morpho-tectonic indices reinforce the observation that both the starting and ending points are tectonically active. Finally, river profiles reveal that the sub-basin's left section displays the most notable river entrenchment, likely due to uplift. Our geomorphic assessment indicates that the Western Ghats within the Cauvery sub-basin region exhibit tectonic activity, characterized by a series of faults along the mountain's leading edge. The presence of Pseudotachylites connected to the fault system indicates that neo-tectonic processes also have an impact on the Shivanasamudra falls, which are situated at the end of the research region.

Keywords: Geomorphic indices, Tectonics, Fault, Morpho-tectonics, Hypsometry.

1. Introduction

Active tectonics is investigated because it serves as a proxy for historical tectonic activity. Now it's easier to find accurate rates of different earth movements like uplift, incision, erosion, and sliding on faults over time, because of new tools in geochronology and geodesy. (Schumm et al., 2000; Burbank and Anderson, 2001; Keller and Pinter, 2002; Bull, 2007; Bull, 2008; Bull 2009 a,b). Rivers are naturally produced surface features that carve out the terrain in any location with a slope in one or more directions. Direction is dynamic and depends on both local and regional terrain. The river forms incisions along its path as a result of differential (gradient) stream power (Brookfield, 1998). Regional or local tectonics, as well as neo-tectonic activity, can all have an impact on the river (Borgohain et.al. 2017). The effect can be slight or severe, changing the path of the river dramatically (Bhattacharjee and Mohanty, 2020). The only way to ascertain how a stream or river pattern has changed is by assessing tectonic/neotectonic activity with geomorphic indices (Zhang et.al., 2019; Miller, et.al. 1953). We can learn about the current tectonic activity by observing the land's shape, the way rivers move, and the height of the area. (Azor et al., 2002; Keller et al., 2000; Molin et al., 2004; Bull, 2007). In areas where the Earth's crust is shifting and moving, the way water flows and forms rivers is easily changed by cracks and bends in the ground. Among other consequences, these processes may result in river diversions, catchment asymmetry, and rapid river incision. (Salvany, 2004; Schoenbohm et al., 2004; Cox, 1994; Jackson et al., 1998; Clark et al., 2004). Tectonic uplift is linked to river incision in these locations, but other processes including Stream piracy, lowering of the base level, and weather events can also lead to rivers cutting through the land in different ways and faster. (Starkel, 2003; Azañón et al., 2005; Hancock and Anderson, 2002). To figure out how fast tectonic and geomorphic processes are happening, scientists use numerical dating on geomorphic surfaces and deposits. (Pérez-Peña et al., 2009; Watchman and Twidale, 2002; Hetzel et al., 2002).

The river sub-basin chosen for tectonic studies is located in the section upstream of Karnataka's Cauvery River Basin (Agrawal et.al., 2022; Anand and Pradhan, 2019). The river travels east from the Brahmagiri forest area's Western Ghats till it reaches Hogenakkal Falls in Karnataka (Vaidyanadhan, 1971). Active and Recent tectonics of quaternary age can be considered as the primary force leading to upliftment in mountain ranges, with their current topography the consequence of erosion and tectonic processes competing (England and Molnar, 1990; Bishop, 2007; Pei et.al., 2021). The sub-basin is located between latitudes 11˚ 54' 27.5"N and 13˚ 19' 59.24"N, and longitudes 75˚ 30'E and 77˚ 38' 57.64"E (Figure 1). The study wants to use geomatics to learn more about how the upper part of the Cauvery River sub-basin, from Talacauvery to Shivanasamudra Falls, has changed in shape and structure (Bhattacharya, 2013), over time, and how tectonic forces have affected the way the river was formed (Das and Saraf, 2007). This study uses geomorphic indices to assess tectonic activity from the Quaternary period in the upper part of the Cauvery sub-basin (Shukla, et.al., 2014).

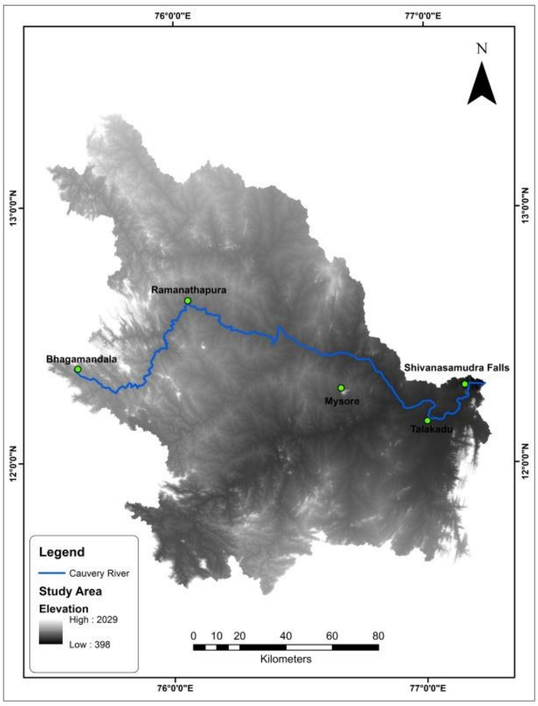

Figure 1. Study area showing nearby important places in the sub-basin (Green Circle)

2. Geological Setting

The Cauvery River begins in the Western Ghats (Subrahmanya, 1987), which have gneissic terrain and low to medium grade metamorphism. The Kabini, an important tributary that demonstrates high grade metamorphism with rock types such as gneiss-derived charnockites, originates in the Southern Granulitic Terrain (SGT) (Talukdar, et.al., 2022) (Taylor et al., 1984). These areas have Precambrian-aged rock types. In addition to a few igneous areas, the rocks have metamorphosed into granulite facies (Nutman et al. 1992). Gneiss and Charnockite can be found combined in Periyapatna, Ramanathapura, Kushalnagara, and other nearby regions (Figure 3).

In addition, the Mysore taluks have a variety of mafic dykes such as Dolerite, Gabbro and Norite. The Chamundi Granite (Srikantappa, et.al., 1992), found nearby, is an igneous pluton that was formed around 800 million years ago. Numerous quartz and pegmatite veins have penetrated the basement rock, which contains migmatites, quartzite, garnet biotite schist, metapelites, younger granites, and felsites (Swaminath and Ramakrishnan, 1981). Greenstone schist belts can also be found in the areas surrounding Karighatta and Srirangapatna, which indicate the end of the Chitradurga greenstone belt (Chadwick, et.al. 2007). The river flows via the Shivanasamudra Falls, Talakadu, Mudukutore, and T. Narasipura to the east. Gneiss, charnockite (Janardhan, et.al. 1982), syenite, and amphibolites can all be found along the river's route. Pseudotachylite (Figure 2) has formed veins in the weak planes and joints right upstream from Shivanasamudra Falls.

Figure 2. Pseudotachylite before the Shivanasamudra falls (Cauvery katte)

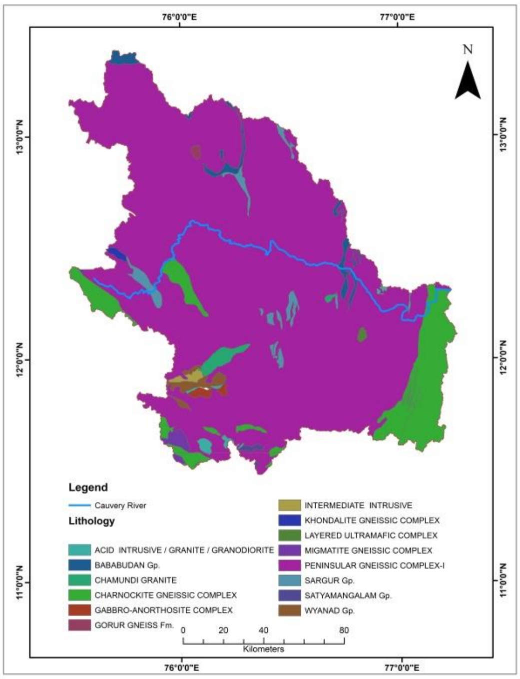

Figure 3. Geological map of the Cauvery River basin (Geological Survey of India, Government of India, 2023)

3. Materials and Methods

The image with the number D43V_V3R1, D43W_V3R1, and D43X_V3R1 Cartosat-1s be downloaded from Bhuvan (ISRO) website, which has a spatial resolution of 2.5m and 30kms swath. The image has 10 bit radiometric resolution. The Cartosat-1 image has been mosaicked and later clipped using study area boundary shapefile.

This cartosat-1 image is used because of its elevation used for analysing morpho-tectonic analysis.

We have looked at several geomorphic indices (Ahmad, 2018), including valley floor width-to-height ratio (Vf), mountain front sinuosity (Smf), asymmetry factor (AF), gradient index of stream length, channel sinuosity index, transverse topographic symmetry, basin elongation ratio, hypsometric curve (Walcott and summerfield, 2008), and basin shape. Tectonic and neo-tectonic activity is indicated by these indices (Kale et.al. 2014).

4. Basin Metrics

The study area, or Cauvery upstream sub-basin, is 21,962 km^2 in size. The terrain's highest point is around 2029 meters, while its lowest point is 398 meters. The sub-basin measures 189 km in length and 252 km in width. Basin relief is the difference in height between the highest and lowest points in a basin. This difference is created by the rocks and structures below, the way the land is built, and how water flows through the area.

5. Results and Discussion

5.1 Morpho-Tectonic Indices

5.1.1 Mountain Front Sinuosity (Smf)

Mountain front sinuosity, or Smf, was defined by Bull in 1977 (Smf=Lmf/Ls) as the ratio between the length of the mountain front at the base of the mountain, where the land slope changes, and the straight-line distance of the mountain front.

Tectonic activity along mountain fronts is assessed by this indicator. (Silva et al., 2003; Keller and Pinter, 2002; Bull and McFadden, 1977; Bull, 2007). Tectonic activity near mountain edges is tracked using this indicator. In areas where mountains are still rising, erosion happens mainly because the land is moving upward, which forms straight edges and leads to lower Smf values. Erosion processes will result in uneven or high Smf values on sinuous fronts on less active fronts (Cheng, et.al., 2016). If the Smf index is less than 1.4, it suggests that the area is part of a tectonically active region, according to several studies. (El Hamdouni et al., 2008; Martín-Rojas et al., 2001; Keller, 1986; Silva et al., 2003).

Smf index for the two adjacent northern mountain fronts in the Cauvery sub-basin was calculated in this study. The values of 1.44 and 0.7 suggest there is moderate to high neo-tectonic activity, which matches up with various tectonic environments. On the other hand, southern mountain front has a mean Smf value of 0.49, indicating a rather high level of neotectonic activity that is consistent with other tectonic and geomorphic characteristics (Figure 4).

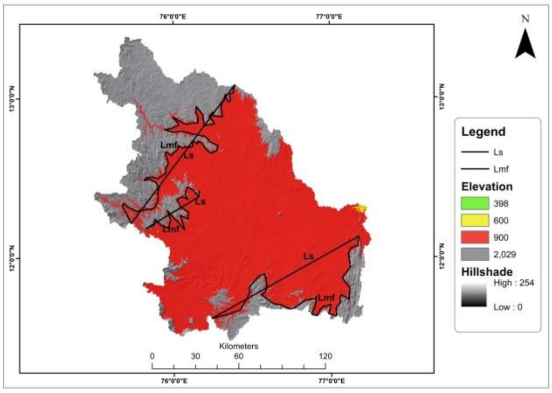

Figure 4. Mountain front sinuosity

5.1.2 Basin Elongation Ratio (Re)

The index is essential for figuring out a basin's form. and provides information on the hydrogeological properties of a drainage area (Schumm, 1956). A drainage basin's elongation ratio shows its most recent tectonic activity. Tectonically active basins are places where the BE value is less than 0.50, meaning they are very active. If the BE value is between 0.50 and 0.85, the basin is considered mildly active. Basins with a BE value higher than 0.85 are classified as dormant (Bull and McFadden, 1977). The Cauvery River sub-basin has an elongation ratio of 0.88 according to this study, which suggests it is experiencing some moderate tectonic activity.

5.1.3 Stream-Length Gradient Index (SL)

When erosion equals height of land, dynamic force equilibrium is achieved. River systems often exhibit a concave longitudinal shape due to balancing (Schumm et al., 1956; Hack, 1973). There are various reasons why the river's profile changes, including lithological and tectonic/neo-tectonic factors (Mishra, et.al, 2016). The index is used to evaluate how environmental factors affect a river's longitudinal profile. This method uses how water moves and shapes the land to find where a stream system settles into balance. Areas where there has been recent tectonic movement are places with softer rocks and higher SL values. High SL values also show that the river is moving over strike-slip faults. Equation gives a mathematical definition of the SL index. $SL = (\Delta H/\Delta Lr)*Lt$, Where $\triangle H$ stands for elevation change, $\triangle Lr$ stands for reach length, and Lt is the distance from the midpoint split of the watershed. Standardized values were used to classify the data, which helps determine the SL value throughout the length of the river and stream (Figure 5).

The shape of the river as it flows and the SL index values show an upward trend in places where there is tectonic activity. The stream-length gradient (SL) index is calculated for the research area. Most of the basin is divided into three main groups: low, moderate, and high. The basin is surrounded by several significant faults, minor faults and lineaments. According to (Keller, 1986; Dehbozorgi et al., 2010), The 21,962 km^2 basin region, which includes the streams that flow along fault zones at Shivanasamudra Falls, is categorized as an active neo-tectonic zone at both the origin and the termination points with lower SL values. Greater SL index values in the places where bigger green dots in SL index map (Figure 5). These might be the knickpoints as a result of tectonic activity (Brookfield, 1998), with thrusts and lithological contrast, a higher SL value indicates tectonic control of the basins. (Sharma and Sarma, 2017).

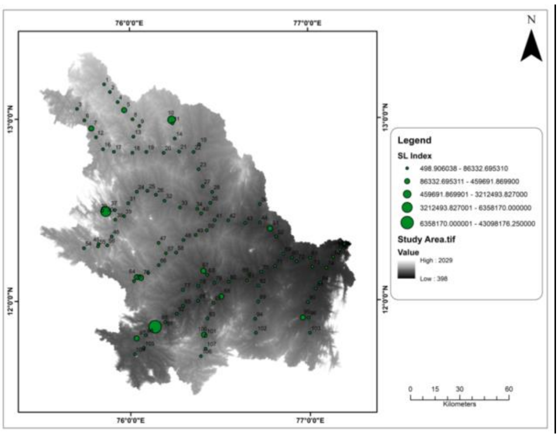

Figure 5. The gradient index for stream length indicates the gradient along the river's path. Green dots show the gradient on the course of the river. Bigger the size greater the gradient (probably knickpoints).

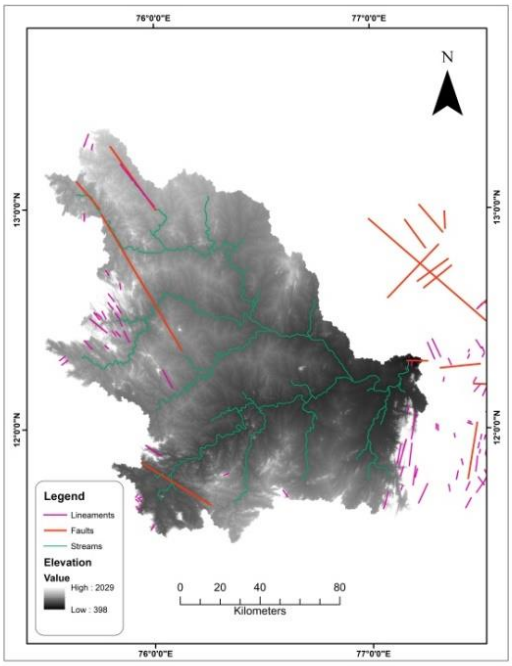

Figure 6. Map showing Faults, Lineaments and Stream network in and around the study area

5.1.4 Valley Floor Width to Valley Height Ratio (Vfh)

The width of the valley floor compared to the height of the valley (Vfh) is a key measure used to tell the difference between V-shaped and U-shaped valleys. It indicates the amount of tectonic activity happening (Bull and McFadden, 1977). The following is a mathematical expression for the index:

$$Vfh = 2Vfw /(Erd - Esc) + (Eld - Esc)$$

The elevations of the right and left valley divides that face downstream are called Erd and Eld. Vfw is the width of the valley floor, and Esc is the average elevation of the valley floor. The Vfh index along a river channel indicates elevation and incision. If the Vfh value is low, it means there is more cutting and lifting happening, which causes the creation of deep V-shaped valleys, since tectonic activity dominates erosional processes (Raj, R., 2012). A high Vfh score indicates a valley that is U-shaped or flat-floored and is mostly the result of bed-level erosional processes. Six cross-sections (AA^{I}, BB^{I}, CC^{I}, DD^{I}, EE^{I}, and FF^{I}) were created for this investigation using the DEM data, and they are displayed in (Figure 7).

In the Eastern Betic Cordillera (southeastern Spain), a similar study by Bull and McFadden (1977) and Silva et al. (2003) shows that wide U-shaped troughs where the Vf value is higher than one indicate significant lateral erosion, These features could be due to simple stability or quiet tectonic activity, while V-shaped valleys with low Vf values under 1 form as a result of active uplift.

The results show the value of 0.26 for AA^{1}, 0.5 for BB^{1}, 1.11 for CC^{1}, 2.43 for DD^{1}, 0.39 for EE^{1}, 0.3 for FF^{1}. Out of all the above values the cross-sections of AA^{1},BB^{1}, EE^{1} and FF^{I}. For the cross-sections AA^{1} (Figure 7a), BB^{1} (Figure 7b), EE^{1} (Figure 7e), and FF^{1} (Figure 7f), the Vfh value is less than 1, which means the area has a V-shaped valley and is in an early stage of basin development. The prevalence of erosional and depositional processes, which result in the formation of broad U-shaped valleys, is indicated by the cross-section CC^{I} (Figure 7c), and DD^{I} (Figure 7d), with Vfh values greater than 1.

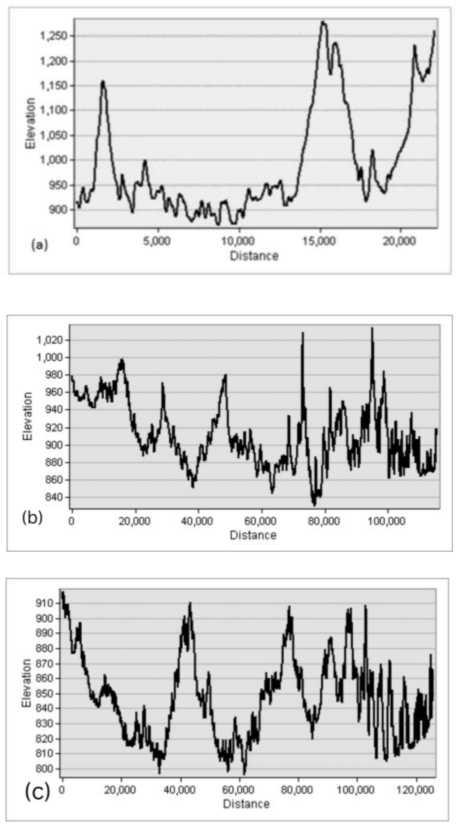

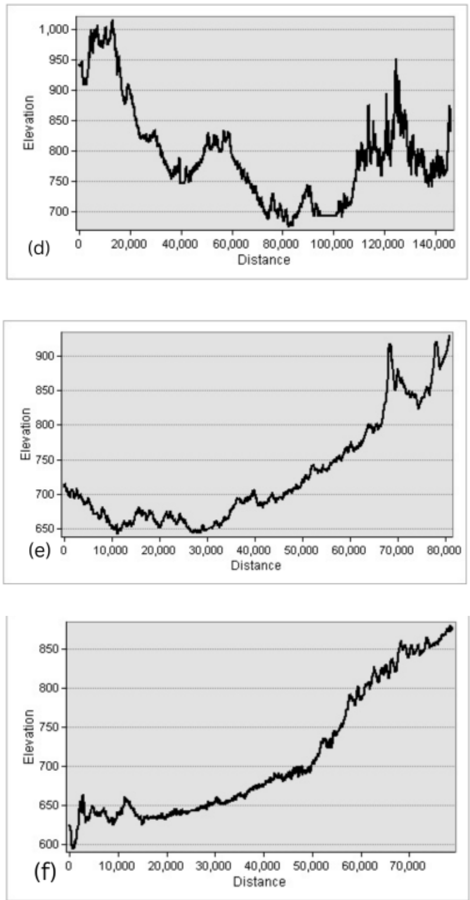

Figure 7. Cross section of valley height to valley floor width [(a) AA^{I} (b) BB^{I} (c) CC^{I} (d) DD^{I} (e) EE^{I} (f) FF^{I}]

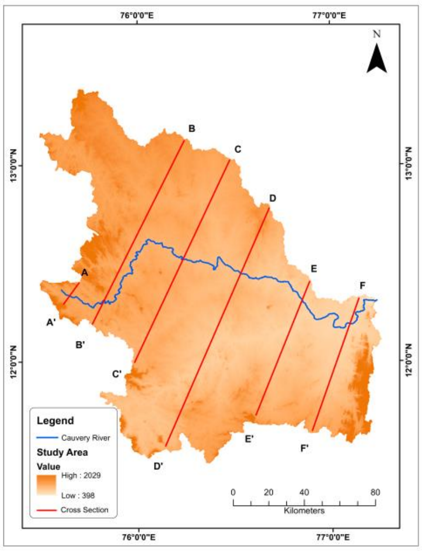

Figure 8. valley height to valley floor width ratio [(a) AA^{I} (b) BB^{I} (c) CC^{I} (d) DD^{I} (e) EE^{I} (f) FF^{I}]

5.1.5 Asymmetric factor (Af)

A crucial component of basin drainage, the asymmetry factor (Af) establishes whether the basin is tectonically tilted or not. The main river flows out from the center of the basin and goes toward the sloped region, which is caused by the movement of tectonic plates. It can be represented and applied both across a wide area and at the basin drainage scale. The formula (Ar/At)*100 = Af is used, where Ar represents the area of the basin to the right of the river downstream. This formula was created by Hare and Gardner in 1985. If the Af value is more or less than 50, it means that tectonic activity or different kinds of rocks are affecting the area. When the Af value is near 50, it means the basin is not tilted much, if at all. Before calculating Af, the areas on both sides of the thalweg line are identified using GIS software. The thalweg line shows the main direction of water flow and helps to identify the sub-basin in the study area. The direction of tilting in the basin is taken into account, and the Af value is calculated as the absolute value of (Af-50) (Figure 9).

The basin's asymmetry helps determine how much it has tilted due to tectonic activity. This study looks at an area of 8,904 km², and there are large faults close to where the river begins on the left side of the basin, which feeds into the main river. These faults show that the area is active tectonically (40.54). The tectonic zone in the center of the basin is moderately active. Because of the faults in the Shivanasamudra Falls area, there is higher neo-tectonic activity on the basin's right side, which is 59.45 and covers 13,057 km². It makes it quite evident that the bulk of the region is located in moderately active tectonic zones, and that two locations, the origin point and the termination point are extremely neo-tectonic. This could be because of the existence of faults and thrusts that run through these basins.

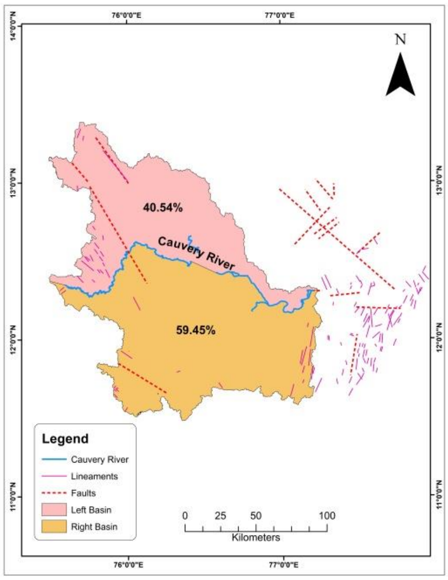

Figure 9. Asymmetric factor showing regional faults and Lineaments

5.1.6 Stream Sinuosity (SS)

Another key sign of tectonic activity in a region is how twisty or winding a stream is. To measure this, we use the stream sinuosity index. This is found by dividing the actual length of a stream by the straight line distance between where the stream starts and ends. In SS, the equation CL = CL divided by L is used to determine what stream length and straight-line distance, as depicted in

(Figure 10). If the SS number is high, it means the river is steady and in balance. A small number indicates significant changes in the area. Tectonic activity is shown when SS is less than 1.05, semi-active when it's between 1.05 and 1.5, and passive when it's above 1.5 (Mueller, 1968; Bull and McFadden, 1977).

This study reveals that the SS index is 1.59. Based on this score, most of the area falls into the low to moderate tectonic activity zone.

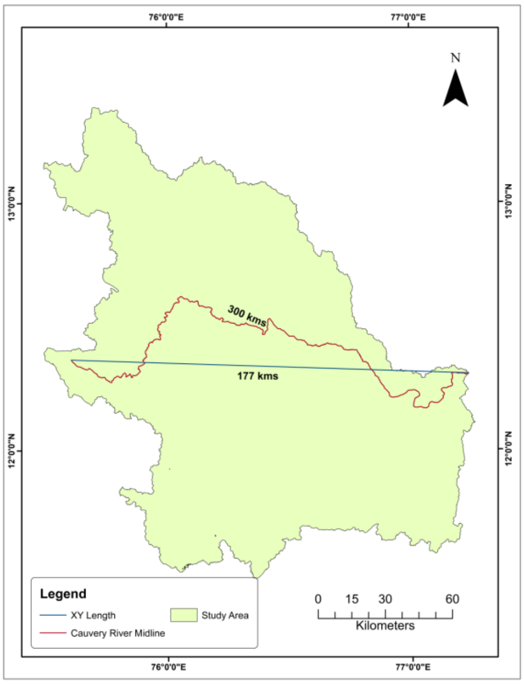

Figure 10. Stream sinuosity

5.1.7 Transverse Topographic Symmetry (T)

The transverse topographic symmetry, or T, is used to show how much a basin has tilted because of tectonic forces. This T value is found by looking at the symmetry vector of the basin, which takes into account how much the meander belt moves away from the middle line of the basin. The T value is between 0 and 1, and it can be calculated using a specific equation.

$T = Da/Dd$

In the equation mentioned above, Da denotes the distance between the stream channel and middle line of a basin, while Dd is the ratio between its division point and the middleline of the basin. When measuring basin tilting caused by tectonic activity, transverse topographic symmetry (T) values are assessed; T > 0 for an asymmetric basin and T = 0 for a symmetric basin. (Cox, 1994). The value of 0 to 0.2 infers the area is less tilted. Value above 0.2 signifies the highly tilted areas.

The T value for the current study is between a minimum of 0.03 and a high of 0.93.The regions in this study with values of 0.23, 0.27, 0.3, 0.22, 0.24, 0.21, 0.42, 0.92, and 0.93 are considered to be highly tilted. Moderate to low tilted zones are represented by the regions with values of 0.11, 0.03 (Figure 11).

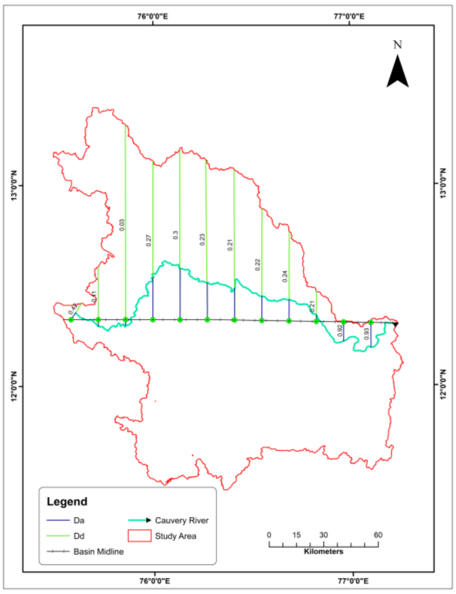

Figure 11. Transverse topographic symmetry

5.1.8 Basin shape (Bs)

The basin shape index is explained in the link provided. (Ramirez-Herrera, 1998; Cannon, 1976). Bs is calculated by dividing the length of the basin from the start to the end (Bl) by the maximum width of the basin (Bw). Tectonic activity is relatively higher in longer basins are typically linked to higher Bs values (>1). A basin with a more circular form and medium values of Bs (0.5<1) suggest moderate tectonic activity. Little Bs values (<0.5) suggest little tectonic activity.

Because tectonic activity and changes in the landscape shape a basin, the basin shape index is used to determine how active the tectonic forces are in that area. Circular basins predominate in areas with little or no tectonic activity, while elongated basins are typically found in areas with active tectonics. The study strongly correlates between the sub-basin's shape and existence of the tectonic features such as lineaments, faults, or thrust. For the sub-basin, the result is 0.7. With the exception of the origin point and the termination point, which have a strongly neo-tectonic zone, based on the basin shape index, the results unequivocally demonstrate that the remaining basin area is experiencing considerable tectonic activity. (Figure 12).

5.1.9 Hypsometric Curve and Integral

This is the part of the basin that remains not disturbed under the hypsometric curve. Topographic map's minimum and maximum altitudes are directly obtained in order to measure HI (Keller and Pinter, 2002).

The hypsometric integral for the current study region is 0.48, These sub-basins are still developing but are comparatively less stable tectonically, as indicated by HI values > 0.30 and < 0.50. The Western Ghats are where the research area starts and ends in Shivanasamudra falls, both of which have extensively dissected landforms. The majority of the terrain in between has a modest slope (Figure 13).

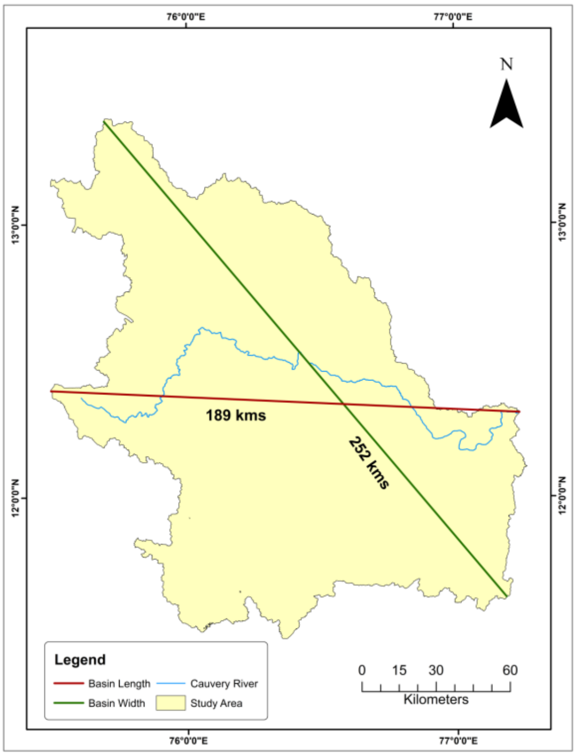

Figure 12. Basin shape

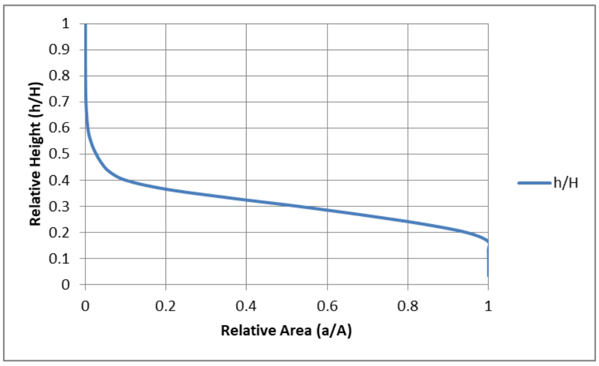

Figure 13. Hypsometric curve of the research area

5.1.10 Longitudinal Profile

The effectiveness of longitudinal profile analysis in determining how rivers react to active tectonic activity is generally acknowledged (Sinha, 2001). Its effectiveness is dependent on the detection of anomalies in channel slope under conditions of disequilibrium, which indicate uplift along active faults, because it shows elevation on the y-axis and distance on the x-axis. According to Wells et al. (1988), an upwardly convex profile denotes Continuous base level lowering and minimal channel downcutting, as well as a shorter time since the base level fell. A profile that goes upward shows older basins and damaged channels because there was more time after the basement dropped lower.

The longitudinal profile is created only for the main Cauvery river. The river at the initial stages has lot of spikes indicating knickpoints showing the highly tectonic nature. Later, there is a gradual drop in the gradient. Next, another steep gradient at chunchanakatte falls, KRS dam can be seen. A major knickpoint and steep gradient is visible at Shivanasamudra falls. All these are majorly because of faults and lineaments.

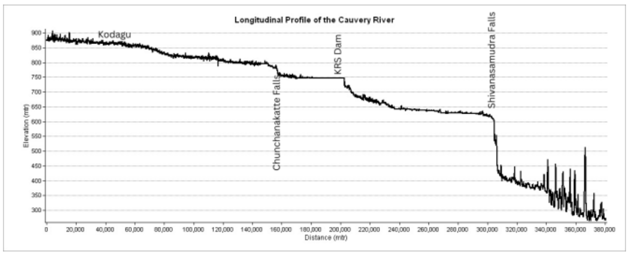

Figure 14. Longitudinal profile of Cauvery river showing knickpoints and gradient.

6. Conclusions

According to the morpho-tectonic indices calculated in this study, the Cauvery upstream sub-basin is moderately tectonically active in the middle part of the basin. At the same time, the starting point in the Western Ghats and the ending point in Shivanasamudra are more active because of new tectonic movements and faults. The Shivanasamudra falls and origin points are the places where heavily dissected hills and valley are present. Mountain front sinuosity (Smf) shows that mountain fronts are active in the south and northwest. These mountain fronts are caused by active NW-SE normal faults in the northwest and E-W transfer strike-slip faults in the south. In both the northern and southern parts of the Cauvery sub-basin, there are active faults that run in the NNE-SSW direction, as shown by the asymmetry indexes from the main catchments. The river's ridge-line and longitudinal profiles, along with the hypsometric curves, show that the Cauvery sub-basin's northern and southern regions have seen increased tectonic activity. The morpho-tectonic markers in this study of the Cauvery sub-basin show active edges on the north and south sides. These edges represent normal faults on the north and transfer strike-slip faults on the south. Uplift of the Western Ghats during the cretaceous period, combined with multiple occurrences of erosion and uplift, resulted in terrace-like structures in the eastern section with a gentle slope especially after chunchanakatte falls upto KRS dam. The river re-enters youth stage by creating a gorge at Shivanasamudra Falls and Mekedatu Falls.

Reference

Agrawal, N., L. Gupta and J. Dixit (2022). Geospatial assessment of active tectonics using SRTM DEM-based morphometric approach for Meghalaya, India. All Earth, 34(1), 39–54.

Ahmad, S., A. Alam, B. Ahmad, A. Afzal, M. I. Bhat, M. S. Bhat and H. F. Ahmad (2018). ‘.Tectono-geomorphic indices of the Erin basin, NE Kashmir valley, India. Journal of Asian Earth Sciences, 151, 16–30.

Anand, A. K. and S. P. Pradhan (2019). Assessment of active tectonics from geomorphic indices and morphometric parameters in part of Ganga basin. Journal of Mountain Science, 16(8), 1943–1961.

Azañón, J. M., A. Azor, J. V. Pérez-Peña and J. M. Carrillo (2005). Late Quaternary large-scale rotational slides induced by river incision: The Arroyo de Gor area (Guadix basin, SE Spain). Geomorphology, 69, 152–168.

Azor, A., E. A. Keller and R. S. Yeats (2002). Geomorphic indicators of active fold growth: South Mountain–Oak Ridge anticline, Ventura basin, southern California. Geological Society of America Bulletin, 114(6), 745–753.

Bhattacharya, F., B. K. Rastogi and G. C. Kothyari (2013). Morphometric evidence of seismicity around Wagad and Gedi Faults, eastern Kachchh, Gujarat. Journal of the Geological Society of India, 81, 113–121.

Bhattacharjee, N. and S. P. Mohanty (2020). GIS-based approach for the measurement of variability in tectonomorphic signatures using DEM data: A case study from the Habo Dome in the Kachchh area, India. Environmental Earth Sciences, 79(18), 1–26.

Bishop, P. (2007). Long-term landscape evolution: Linking tectonics and surface processes. Earth Surface Processes and Landforms, 32, 329–365.

Borgohain, S., J. D. Das, A. K. Saraf, G. Singh and S. S. Baral (2017). Structural controls on topography and river morphodynamics in Upper Assam Valley, India. Geodinamica Acta, 29(1), 62–69. https://doi.org/10.1080/09853111.2017.1313090

Brookfield, M. E. (1998). The evolution of the great river systems of southern Asia during the Cenozoic India–Asia collision: Rivers draining southwards. Geomorphology, 22(3–4), 285–312.

Bull, W. B. (1977). Tectonic geomorphology of the Mojave Desert, California. U.S. Geological Survey Contract Report 14-0-001-G-394, Office of Earthquakes, Volcanoes, and Engineering, Menlo Park, California, pp. 188.

Bull, W. B. and L. D. McFadden (1977). Tectonic geomorphology north and south of the Garlock fault, California. In Doehring, D. O. (ed.) Geomorphology in Arid Regions: Proceedings of the Eighth Annual Geomorphology Symposium. State University of New York, Binghamton, NY, pp. 115–138.

Bull, W. B. (2007). Tectonic Geomorphology of Mountains: A New Approach to Paleoseismology. Wiley-Blackwell, Oxford, pp. 328.

Bull, W. B. (2008). Tectonic Geomorphology of Mountains: A New Approach to Paleoseismology. John Wiley and Sons.

Bull, W. B. (2009a). Tectonically Active Landscapes. Wiley-Blackwell, Oxford, pp. 326.

Bull, W. B. (2009b). Geomorphic Responses to Climatic Change. Blackburn Press, New Jersey, pp. 326.

Burbank, D. W. and R. S. Anderson (2001). Tectonic Geomorphology. Blackwell Science. 254–356.

Cannon, M. (1976). Blind deconvolution of spatially invariant image blurs with phase. IEEE Transactions on Acoustics, Speech, and Signal Processing, 24(1), 58–63.

Chadwick, B., V. N. Vasudev, G. V. Hegde and A. P. Nutman (2007). Structure and SHRIMP U/Pb zircon ages of granites adjacent to the Chitradurga schist belt: Implications for Neoarchaean convergence in the Dharwar craton, southern India. Journal of the Geological Society of India, 69.

Cheng, W., N. Wang, M. Zhao and S. Zhao (2016). Relative tectonics and debris flow hazards in the Beijing Mountain area from DEM-derived geomorphic indices and drainage analysis. Geomorphology, 257, 134–142.

Clark, M. K., L. M. Schoenbohm, L. H. Royden, K. X. Whipple, B. C. Burchfiel, X. Zhang, W. Tang, E. Wang and L. Chen (2004). Surface uplift, tectonics, and erosion of eastern Tibet from large-scale drainage patterns. Tectonics, 23.

Cox, R. T. (1994). Analysis of drainage-basin symmetry as a rapid technique to identify areas of possible Quaternary tilt-block tectonics: An example from the Mississippi Embayment. Geological Society of America Bulletin, 106(5), 571–581.

Das, J. D. and A. K. Saraf (2007). Remote sensing in mapping of Brahmaputra/Jamuna River channel pattern and its relation to various landforms and tectonic environment. International Journal of Remote Sensing, 28, 3619–3631.

Dehbozorgi, M., M. Pourkermani, M. Arian, A. A. Matkan, H. Motamedi and A. Hosseiniasl (2010). Quantitative analysis of relative tectonic activity in the Sarvestan area, central Zagros, Iran. Geomorphology, 121(3–4), 329–341.

El Hamdouni, R., C. Irigaray, T. Fernández, J. Chacón and E. A. Keller (2008). Assessment of relative active tectonics, southwest border of the Sierra Nevada (southern Spain). Geomorphology, 96(1–2), 150–173.

England, P. and P. Molnar (1990). Surface uplift, uplift of rock, and exhumation of rocks. Geology, 18, 1173–1177.

Hack, J. T. (1973). Stream-profile analysis and stream-gradient index. Journal of Research of the U.S. Geological Survey, 1(4), 421–429.

Hancock, G. S. and R. S. Anderson (2002). Numerical modeling of fluvial strath-terrace formation in response to oscillating climate. Geological Society of America Bulletin, 114, 1131–1142.

Hare, P. W. and T. W. Gardner (1985). Geomorphic indicators of vertical neotectonism along converging plate margins, Nicoya Peninsula, Costa Rica. in Morisawa, M. and Hack, J. T. (eds.) Tectonic Geomorphology: Proceedings of the 15th Annual Binghamton Geomorphology Symposium. Allen and Unwin, Boston, pp. 75–104.

Hetzel, R., S. Niedermann, S. Ivy-Ochs, P. W. Kubik, M. X. Tao and B. Gao (2002). Ne-21 versus Be-10 and Al-26 exposure ages of fluvial terraces: The influence of crustal Ne in quartz. Earth and Planetary Science Letters, 201, 575–591.

Jackson, J., R. Van Dissen and K. Berryman (1998). Tilting of active folds and faults in the Manawatu region, New Zealand: Evidence from surface drainage patterns. New Zealand Journal of Geology and Geophysics, 41, 377–385.

Janardhan, A. S., R. C. Newton and E. C. Hansen (1982). The transformation of amphibolite facies gneiss to charnockite in southern Karnataka and northern Tamil Nadu, India. Contributions to Mineralogy and Petrology, 79, 130–149.

Kale, V. S., S. Sengupta, H. Achyuthan and M. K. Jaiswal (2014). Tectonic controls upon Kaveri River drainage, cratonic Peninsular India: Inferences from longitudinal profiles, morphotectonic indices, hanging valleys and fluvial records. Geomorphology, 227, 153–165.

Keller, E. A. (1986). Investigation of active tectonics: Use of surficial earth processes. Active Tectonics, 1, 136–147.

Keller, E. A., D. B. Seaver, D. L. Laduzinsky, D. L. Johnson and T. L. Ku (2000). Tectonic geomorphology of active folding over buried reverse faults: San Emigdio Mountain front, southern San Joaquin Valley, California. Geological Society of America Bulletin, 112(1), 86–97.

Keller, E. A. and N. Pinter (eds.) (2002). Active Tectonics: Earthquakes, Uplift, and Landscape, 2nd edn. Prentice Hall, Upper Saddle River, N.J., pp. 362.

Martín-Rojas, I., M. Martín-Martín and C. Sanz de Galdeano (2001). Índices geomorfológicos de los frentes montañosos del borde occidental de Sierra Nevada (Granada — España). In Pelaez Montilla, J. and López Garrido, A. C. (eds.) La Cuenca de Granada, in Sanz de Galdeano, C. (ed.) Estructura, Tectónica Activa, Sismicidad, Geomorfología y Dataciones Existentes. Universidad de Granada, Granada, pp. 59–66.

Mayer, L. (1990). Introduction to Quantitative Geomorphology. Prentice Hall, Englewood Cliffs, NJ.

Miller, V. C. (1953). A quantitative geomorphic study of drainage basin characteristics in the Clinch Mountain area, Virginia and Tennessee. Technical Report No. 3, Columbia University, New York.

Mishra, R. L., R. Jayangondaperumal and H. Sahoo (2016). Active tectonics of Dikrong Valley, northeast Himalaya, India: Insight into the differential uplift and fold propagation from river profile analysis. Himalayan Geology, 37(2), 85–94.

Molin, P., F. J. Pazzaglia and F. Dramis (2004). Geomorphic expression of active tectonics in a rapidly-deforming forearc, Sila massif, Calabria, southern Italy. American Journal of Science, 304(7), 559–589.

Mueller, J. E. (1968). An introduction to the hydraulic and topographic sinuosity indexes. Annals of the Association of American Geographers, 58(2), 371–385.

Nutman, A. P., B. Chadwick, M. Ramakrishnan and M. N. Viswanatha (1992). SHRIMP U-Pb ages of detrital zircon in Sargur supracrustal rocks in western Karnataka, southern India. Journal of the Geological Society of India, 39(5), 367–374.

Pei, Y., H. Qiu, S. Hu, D. Yang, Y. Zhang, S. Ma and M. Cao (2021). Appraisal of tectonic-geomorphic features in the Hindu Kush-Himalayas. Earth and Space Science, e2020EA001386.

Pérez-Peña, J. V., J. M. Azañón and A. Azor (2009). CalHypso: An ArcGIS extension to calculate hypsometric curves and their statistical moments – Applications to drainage basin analysis in SE Spain. Computers and Geosciences, 35, 1214–1223.

Peucat, J. J., H. Bouhallier, C. M. Fanning and M. Jayananda (1995). ‘Age of the Holenarsipur greenstone belt: Relationships with the surrounding gneisses (Karnataka, South India). The Journal of Geology, 103(6), 701–710.

Raj, R. (2012). Active tectonics of NE Gujarat (India) by morphometric and morphostructural studies of Vatrak River basin. Journal of Asian Earth Sciences, 50, 66–78.

Ramírez-Herrera, M. T. (1998). Geomorphic assessment of active tectonics in the Acambay Graben, Mexican Volcanic Belt. Earth Surface Processes and Landforms, 23(4), 317–332.

Salvany, J. M. (2004). Tilting neotectonics of the Guadiamar drainage basin, SW Spain. Earth Surface Processes and Landforms, 29, 145–160.

Schumm, S. A. (1956). Evolution of drainage systems and slopes in badlands at Perth Amboy, New Jersey. Geological Society of America Bulletin, 67(5), 597–646.

Schumm, S. A., J. F. Dumont and J. M. Holbrook (2000). Active Tectonics and Alluvial Rivers. Cambridge University Press.

Schoenbohm, L. M., K. X. Whipple, B. C. Burchfiel and L. Chen (2004). Geomorphic constraints on surface uplift, exhumation, and plateau growth in the Red River region, Yunnan Province, China. Geological Society of America Bulletin, 116, 895–909.

Sharma, S. and J. N. Sarma (2017). Application of drainage basin morphotectonic analysis for assessment of tectonic activities over two regional structures of northeast India. Journal of the Geological Society of India, 89(3), 271–280.

Shukla, D. P., C. S. Dubey, A. S. Ningreichon, R. P. Singh, B. K. Mishra and S. K. Singh (2014). GIS-based morpho-tectonic studies of Alaknanda river basin: A precursor for hazard zonation. Natural Hazards, 71(3), 1433–1452.

Silva, P. G., J. L. Goy, C. Zazo and T. Bardají (2003). Fault-generated mountain fronts in southeast Spain: Geomorphologic assessment of tectonic and seismic activity. Geomorphology, 50, 203–225.

Sinha, S. R. (2001). Neotectonic significance of longitudinal river profiles: An example from the Banas drainage basin, Rajasthan. Journal of the Geological Society of India, 58, 143–156.

Srikantappa, C., K. P. Narasimha and H. T. Basavarajappa (1992). Highly saline fluid inclusions in

Chamundi granite, South India. Current Science, 62(3), 307–309.

Starkel, L. (2003). Climatically controlled terraces in uplifting mountain areas. Quaternary Science Reviews, 22, 2189–2198.

Subrahmanya, K. R. (1987). Evolution of the Western Ghats, India – A simple model. Journal of the Geological Society of India, 29(4), 446–449.

Swaminath, J. and M. Ramakrishnan (eds.) (1981). Early Precambrian Supracrustals of Southern Karnataka. Geological Survey of India Memoirs, 112, pp. 350.

Talukdar, M., T. Sarkar, P. Sengupta and D. Mukhopadhyay (2022). The Southern Granulite Terrane, India: The saga of over 2 billion years of Earth's history. Earth-Science Reviews, 232.

Taylor, B. E., M. C. Wheeler and D. K. Nordstrom (1984). Stable isotope geochemistry of acid mine drainage: Experimental oxidation of pyrite. Geochimica et Cosmochimica Acta, 48(12), 2669–2678.

Vaidyanadhan, R. (1971). Evolution of the drainage of Cauvery in South India. Journal of the Geological Society of India, 12(1), 14–23.

Walcott, R. C. and M. A. Summerfield (2008). Scale dependence of hypsometric integrals: An analysis of southeast African basins. Geomorphology, 96(1–2), 174–186.

Watchman, A. L. and C. R. Twidale (2002). Relative and absolute dating of land surfaces. Earth-Science Reviews, 58, 1–49.

Wells, S. G., T. F. Bullard, T. M. Menges, P. G. Drake, P. A. Karas, K. I. Kelson, J. B. Ritter and J. R. Wesling (1988). Regional variations in tectonic geomorphology along segment convergent plate boundary, Pacific coast of Costa Rica. Geomorphology, 1, 239–265.

Zhang, T., S. Fan, S. Chen, S. Li and Y. Lu (2019). Geomorphic evolution and neotectonics of the Qianhe River Basin on the southwest margin of the Ordos Block, North China. Journal of Asian Earth Sciences, 176, 184–195.